PHILOSOPHICAL TRANSACTIONS OF THE ROYAL SOCIETY A MATHEMATICAL, PHYSICAL & ENGINEERING SCIENCES

High Resolution Spectroscopy of Narrow Band Giant Pulse Lasers: Time-Dependent Frequency Shifts in Ruby

D. J. Bradley, M. S. Engwell, A. W. McCullough, G. Magyar and M. C. Richardson

Phil. Trans. R. Soc. Lond. A 1968 **263**, 225-237
doi: 10.1098/rsta.1968.0013

HIGH RESOLUTION SPECTROSCOPY OF NARROW BAND GIANT PULSE LASERS: TIME-DEPENDENT FREQUENCY SHIFTS IN RUBY

By D. J. BRADLEY*, M. S. ENGWELL* and A. W. McCULLOUGH*

Department of Physics, Royal Holloway College, University of London, Englefield Green, Surrey

and G. MAGYAR and M. C. RICHARDSON†

Royal Holloway College and U.K.A.E.A. Culham Laboratory, Culham, Berkshire

(*Communicated by S. Tolansky, F.R.S.—Received* 4 *December* 1967—*Read* 23 *May* 1968)

[Plates 3 to 6]

CONTENTS

Both plane and defocused spherical Fabry–Pérot interferometers, with a limiting resolution of less than 10 MHz, have been employed to study the output spectral brightness of narrow band giant pulse ruby lasers. Rotating prism and Pockels cell *Q*-switched systems have been compared and the mode selection properties of resonant reflectors demonstrated. The advantages of uniform pumping of the laser rod, when combined with a dye solution isolator, are illustrated by interferograms showing the direct spectroscopic detection of pure transverse mode structure in giant pulse lasers.

To elucidate apparent discrepancies between time integrated interferograms and pulse envelope beat patterns, time resolved spectroscopy with a fast image tube streaking camera was carried out. Time and intensity dependent blue and red frequency shifts were detected and measured and rapid (< 10 ns) transverse changes of the active region of the ruby were revealed by streaked photographs of the beam cross-section. These results are qualitatively accounted for in terms of the combined effects of rapid bleaching of the central region of an inhomogeneous distribution of population inversion, and nonlinear anomalous dispersion in the ruby. Beam spreading or narrowing with the preferential growth of higher or lower frequency transverse modes respectively then results. Disagreement between theoretical and measured durations of laser giant pulses is thus explained. Beat patterns are shown to be inadequate for the determination of mode structures.

Such frequency shifts (about 200 MHz for a 35 ns 5 MW pulse) seriously limit the time integrated spectral brightness obtainable from giant pulse ruby lasers. A method of reducing them to increase spectral brightness is briefly discussed.

* Now at Department of Pure and Appled Physics, Queen's University, Belfast.
† Now at National Research Council, Ottawa, Canada.

Introduction

For plasma diagnostics by laser scattering (rapidly becoming a standard diagnostic technique) (Evans, Forrest & Katzenstein 1967) and for pulsed laser holography (Fritzler & Marom 1967) high power giant pulse lasers with narrow spectral outputs are required. More generally, a precise knowledge of the optical-frequency electric field strength is necessary for the quantitative interpretation of nonlinear optics experiments involving the interaction of intense laser beams with matter. Such high power lasers generally emit a complex spectrum of longitudinal and transverse modes (Bradley, de Silva, Evans & Forrest 1963) and the resulting spatial and temporal interference of the modes with one another leads to corresponding fluctuations in the optical frequency electric field strength. Thus there was a need for the development both of spectrally pure, high power, laser systems, and of the spectroscopic and other techniques for simultaneously monitoring the laser beam parameters.

Only interferometers are capable of providing the necessary spectral resolving powers exceeding 10^6. Time-resolved spectroscopy in the nanosecond region is also required (the duration of a laser giant pulse is typically less than 50 ns), and, since the time and spectral resolution limits sets by the laser source itself cannot be achieved with spectral scanning by time-sequential variation of the interferometer optical path difference (Bradley, Bates, Juulman & Majumdar 1964), electron-optical image streaking of etalon interferograms has to be employed. A general investigation of the spectral purity of narrow band giant pulse ruby lasers (hereafter designated GPRL), based on these diagnostic techniques, was undertaken and initial results were briefly described at the C.I.O. VII Conference (Paris 1966). The direct spectral detection, from defocused spherical Fabry–Pérot interferograms, of single transverse modes of giant pulse ruby lasers (Bradley, Engwell, McCullough, Magyar & Richardson 1966*a*) and of a time and intensity dependent frequency shift (Bradley, Magyar & Richardson 1966*b*) have since been reported.

In the first reported single longitudinal mode operation of a GPRL (McClung & Weimer 1965) the measured spectral linewidth of 200 MHz was much greater than the corresponding spectral transform of the pulse width measurement. Later a single transverse mode, passive Q-switched ruby laser, employing spherical mirrors was described (Daneu, Sacchi & Svelto 1966) but in this case the evidence for single transverse mode operation was based on the observation of pure near-field mode patterns. The high resolving powers exceeding 10^7, easily obtainable from spherical Fabry–Pérot interferograms (Bradley 1967), are sufficient to spectrally resolve single transverse modes, the separations of which are increased due to refractive index inhomogeneities in the pumped ruby (Stickley 1964). Employing both plane (FPP) and defocused spherical (DFPS) Fabry–Pérot interferometers, we have studied in detail the output spectra of narrow-band ruby lasers, Q-spoiled by rotating prism (Bradley *et al.* 1966*a*) and Pockels cell plus bleachable dye arrangements, respectively. Cavities with spherical and plane mirrors, and various combinations including resonant plate reflectors, have also been studied. We now wish to summarize, and discuss the significance of our results with these moderate power ($\leqslant$ 50 MW) narrow band ($\leqslant$ 500 MHz $=$ 0·017 cm^{-1}) GPRL oscillator systems.

Diagnostics

Spectral analysis

The relative advantages and disadvantages of FPP and DFPS interferograms for giant pulse laser spectroscopy are described in the preceding paper (Bradley & Mitchell 1968) together with details of the design, construction and methods of employing spherical etalons to produce quasi-linear dispersion interferograms. The results described in the present paper were obtained either with a plane interferometer and a fixed gap or with spherical interferometers whose mirrors (polished identically spherical to $\lambda/75$ over their central 0·5 cm diameter region) were separated by a distance, 200 μm less than their 10 cm radius of curvature. With multilayer dielectric mirrors of greater than 98% reflectivity, a reflection finesse of *ca.* 90, corresponding to a spectral resolution limit of less than 10 MHz (free spectral range 750 MHz) is obtainable with a spatially coherent laser beam.

Small gap plane interferometers were employed to check on any overlapping of orders in the DFPS interferograms and for the broader laser spectra. Time resolution in the nanosecond region was obtained by streaking DFPS interferograms, employing a gated image intensifier camera (STL) to produce simultaneously spectral, spatial and temporal resolutions.

Other diagnostics and general experimental arrangements

Time variation of the laser light intensity and modulations arising from beats between modes were detected by a fast photodiode, and recorded on a wideband oscilloscope. Image tube streak photographs of near-field patterns provided information on the time development of laser filaments and transverse mode patterns.

The output of the particular laser system being investigated (figure 1) was monitored via a 1% reflecting beam splitter B_1 (the laser beam is linearly polarized in the plane of the diagram) by a calibrated ITT biplanar photodiode, P, and a Tektronix 519 oscilloscope, of combined passband 1 GHz. A second beam splitter B_2 sampled a few percent of the laser beam for the 10 cm DFPS interferometer. The remainder of the beam was scattered by a diffusing screen S into a variable gap FPP. The plane interferometer was necessary to investigate the total width of the emitted spectrum as a function of pumping energy and for particular cavity arrangements. When optimum spectral performance was achieved the main beam was used for energy measurements, by absorption in a calorimeter, or for beam divergence measurements, by photographing the far field pattern in the focal plane of a long focal length lens through a range of neutral density filters. Since for most applications it is the spectral brightness (power per unit solid angle per unit frequency interval) that is important, simultaneous measurement of spectrum and beam divergence is essential if quantitative comparisons are to be made.

The d.c. excited He—Ne gas laser was employed as a reference beam for setting up the optical system and to calibrate the interferometers. The beam splitter arrangement, B_3 and B_4, made the two laser beams (ruby and He—Ne) collinear. This was essential for correct alinement of the DFPS.

Polaroid type film was employed for initial experimental runs and for very low power beams but otherwise final interferograms were recorded on standard photographic films.

PHILOSOPHICAL TRANSACTIONS OF THE ROYAL SOCIETY A MATHEMATICAL, PHYSICAL & ENGINEERING SCIENCES

Laser Q-switching systems investigated

Three different types of GPRL were studied. Preliminary work with a Kerr-cell switched laser confirmed that it was not suitable for high spectral purity operation due to the presence of satellite lines *ca.* 0·5 cm^{-1} away from the laser line (Hellwarth 1966). At higher power levels a cascaded series of equally spaced Stokes and anti-Stokes components begin to appear. In addition the beam divergence of a Kerr-cell switched laser is considerably greater than other systems. While the satellite component could in general be suppressed by employing a resonant reflector (see below) the resulting spectral brightness produced by a particular ruby rod was less than that achieved with the other forms of Q-switching.

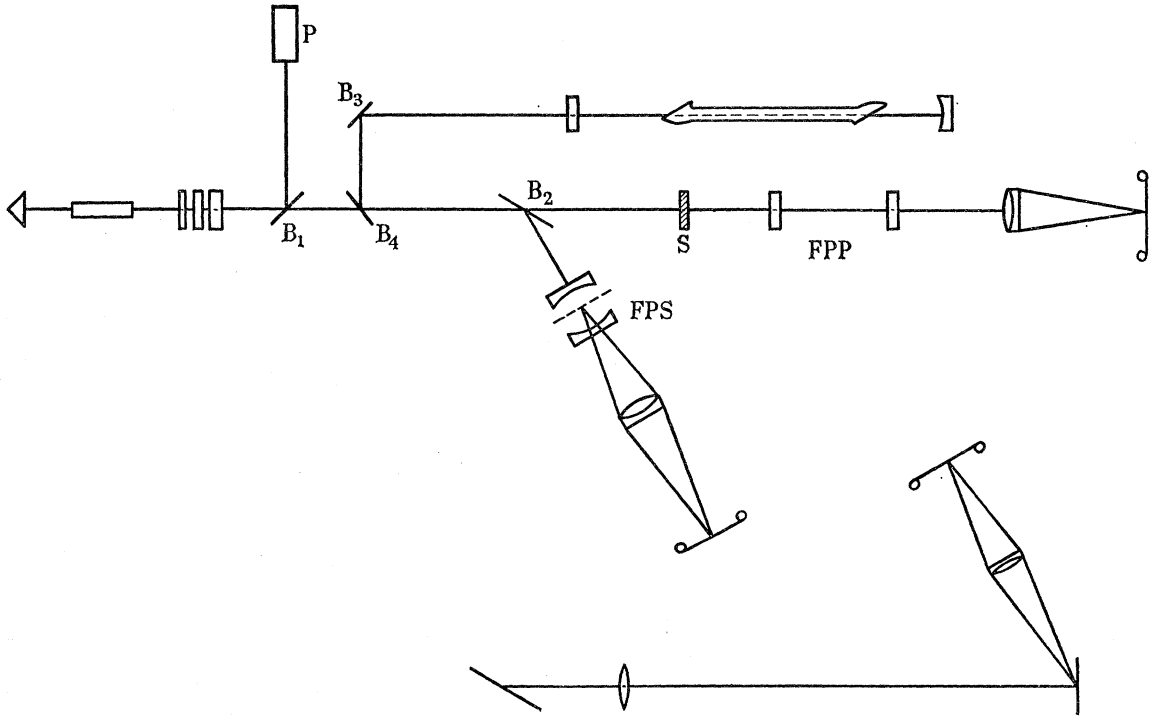

Figure 1. General arrangement for direct spectroscopic detection of narrow-band giant pulse laser outputs.

(i) *Rotating prism GPRL*

This, the first system investigated, consisted of a polished 3 in. × $\frac{3}{8}$ in. ruby rod with plane parallel ends, and pumped ex-focally by a matching linear flash-tube in an elliptical cylindrical cavity. The reflector cavity was lined with polished stainless steel strip overcoated with aluminium. The output mirror had *ca.* 68 % reflectivity. The effective cavity length was 200 cm and peak output powers of 10 to 20 MW were obtained for 600 to 800 joule inputs.

(ii) *Gain switched rotating prism GPRL* (Bradley *et al.* 1966*c*)

A Brewster angled rotating prism coupled two independently pumped ruby rods (6 in. × $\frac{3}{8}$ in. polished and 5 in. × $\frac{3}{8}$ in. fine ground) into a single laser cavity. Both rubies had Brewster angled ends and were optically pumped in the same way as in

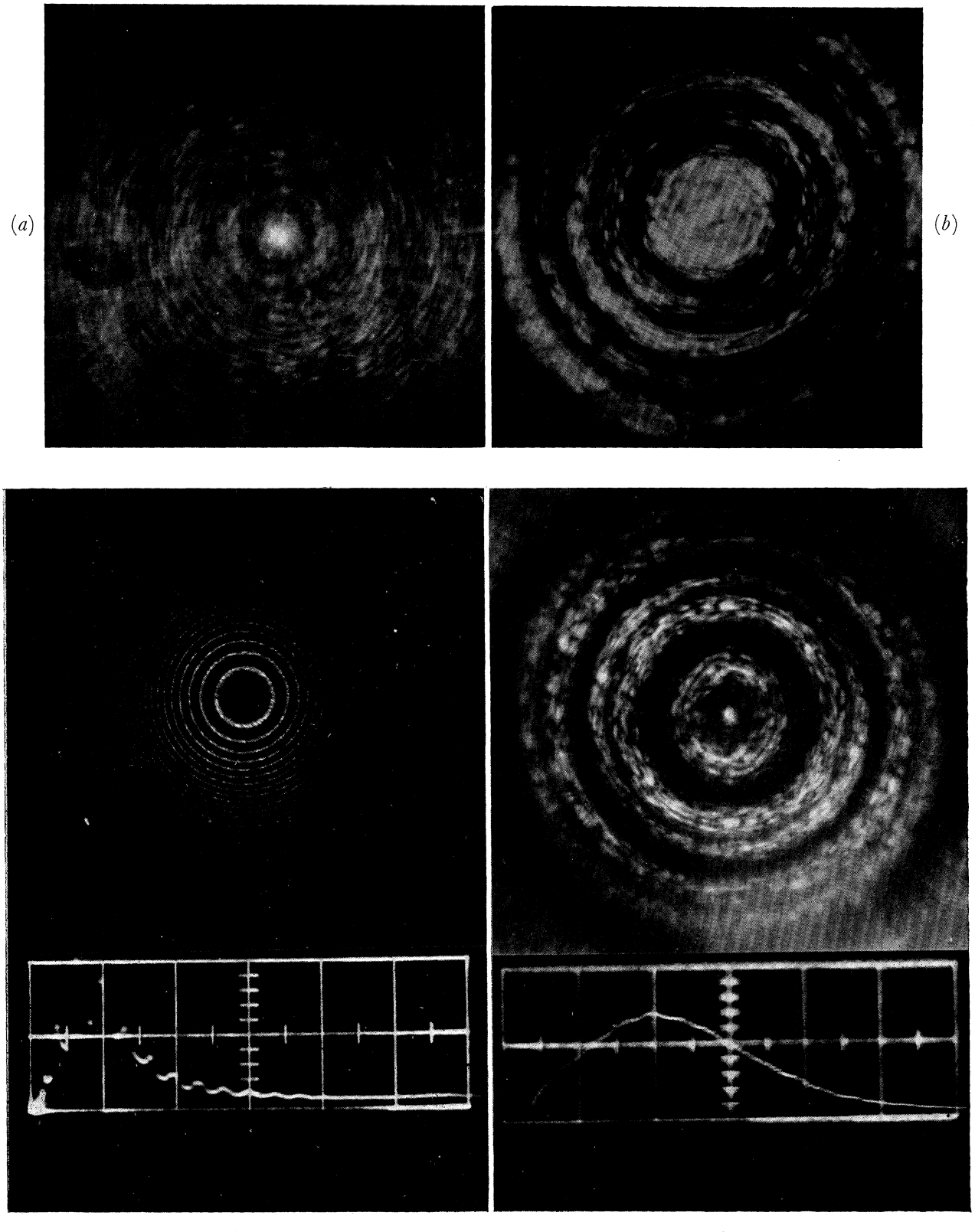

FIGURE 5. (*a*, *b*). Comparison of the spectra of a rotating prism *Q*-switched GPRL taken with a spherical Fabry–Pérot interferometer for (*a*) 68 % reflectivity dielectric mirror (*b*) resonant reflector of same reflectivity. (*c*) Output spectrum of gain-switched rotating prism GPRL. Plane Fabry–Pérot interferogram. Free spectral range 1500 MHz. Oscillogram time scale 20 ns cm^{-1}. Peak power 40 MW. (*d*) Output spectrum of rotating prism system (i) FPS Interferogram. (Free spectral range 750 MHz.) Oscillogram time scale 20 ns cm^{-1}. Peak power 3 MW.

(*Facing p.* 228)

PHILOSOPHICAL TRANSACTIONS OF THE ROYAL SOCIETY A MATHEMATICAL, PHYSICAL & ENGINEERING SCIENCES

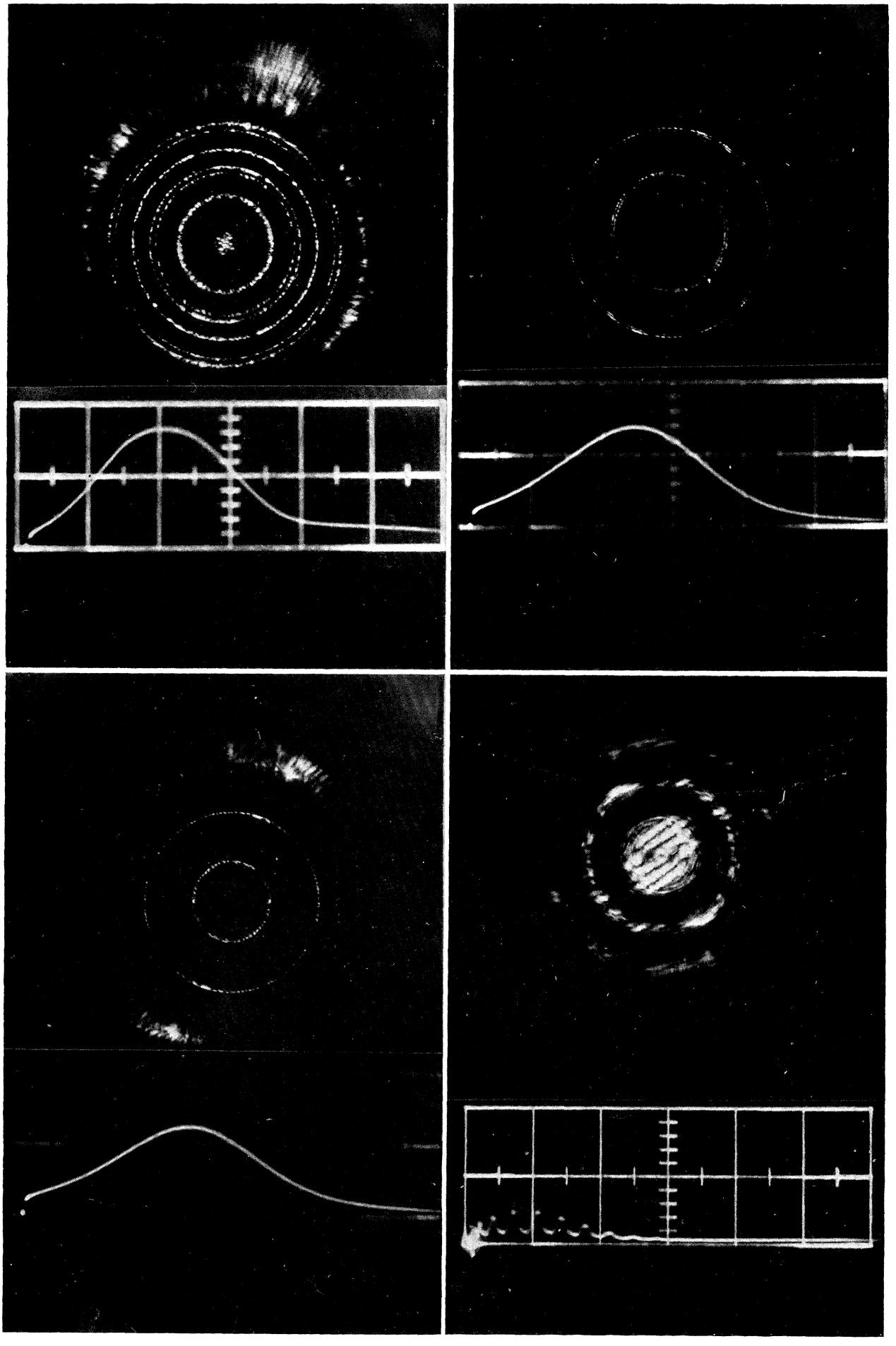

FIGURE 6. (*a*) to (*c*). Output spectra of Pockel's cell *Q*-switched GPRL. DFPS interferograms. Oscillograms time scale 100 ns cm^{-1}. Peak powers $\sim$ 100 kW. (*d*) DFPS interferogram of gain-switched rotating prism GPRL. Oscillogram time scale 20 ns cm^{-1}. Peak power 11 MW.

PHILOSOPHICAL TRANSACTIONS OF THE ROYAL SOCIETY A MATHEMATICAL, PHYSICAL & ENGINEERING SCIENCES

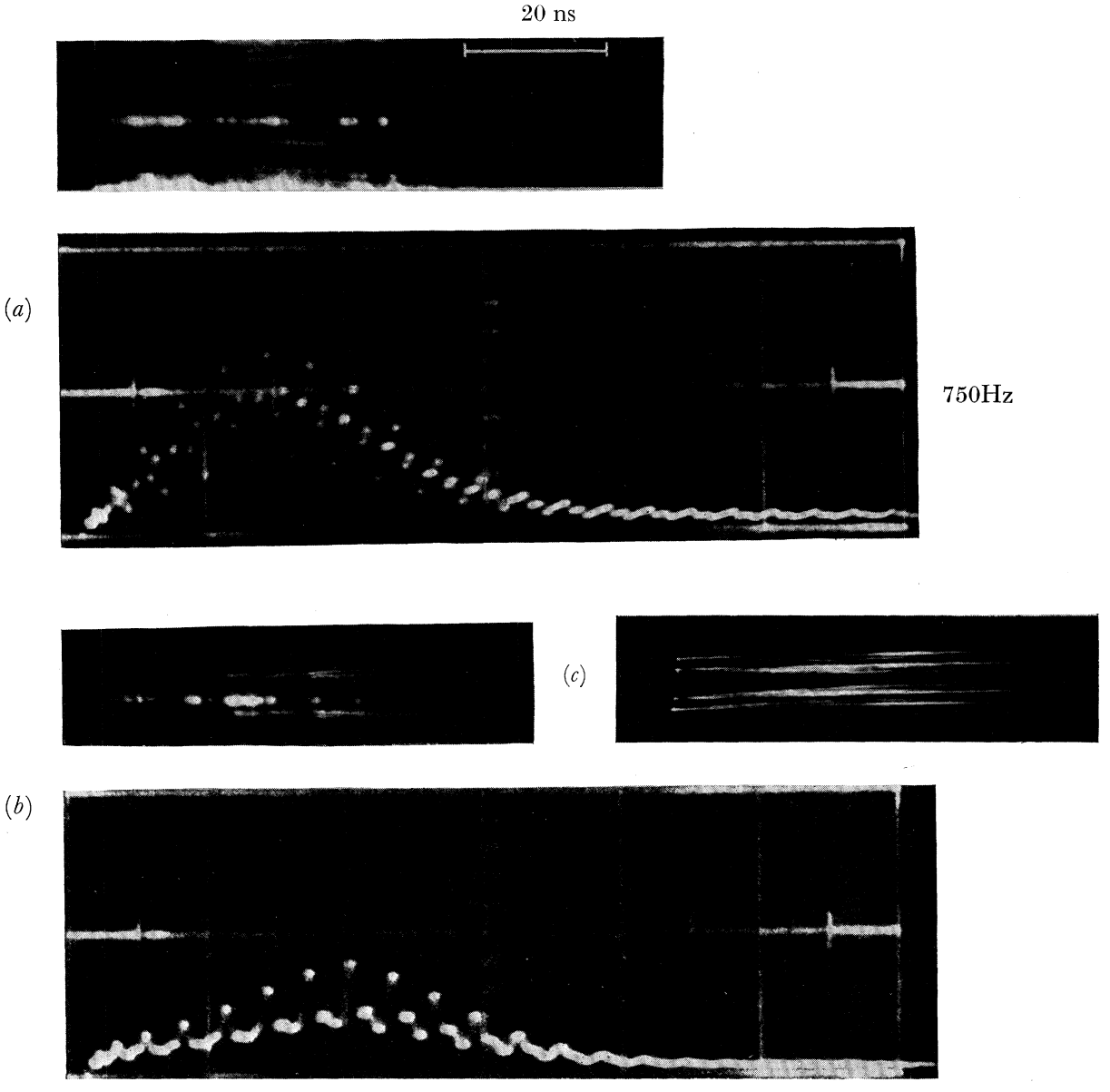

FIGURE 7. Streaked DFPS interferograms of (*a*, *b*) gain switched GPRL. Streak writing rate 2 ns mm^{-1}. Peak output powers (*a*) 4 MW, (*b*) 2 MW. Oscillogram time scale 20 ns cm^{-1}. (*c*) Pockel's cell GPRL. Peak output power 2 MW. Total streak time 200 ns.

PHILOSOPHICAL TRANSACTIONS OF THE ROYAL SOCIETY A MATHEMATICAL, PHYSICAL & ENGINEERING SCIENCES

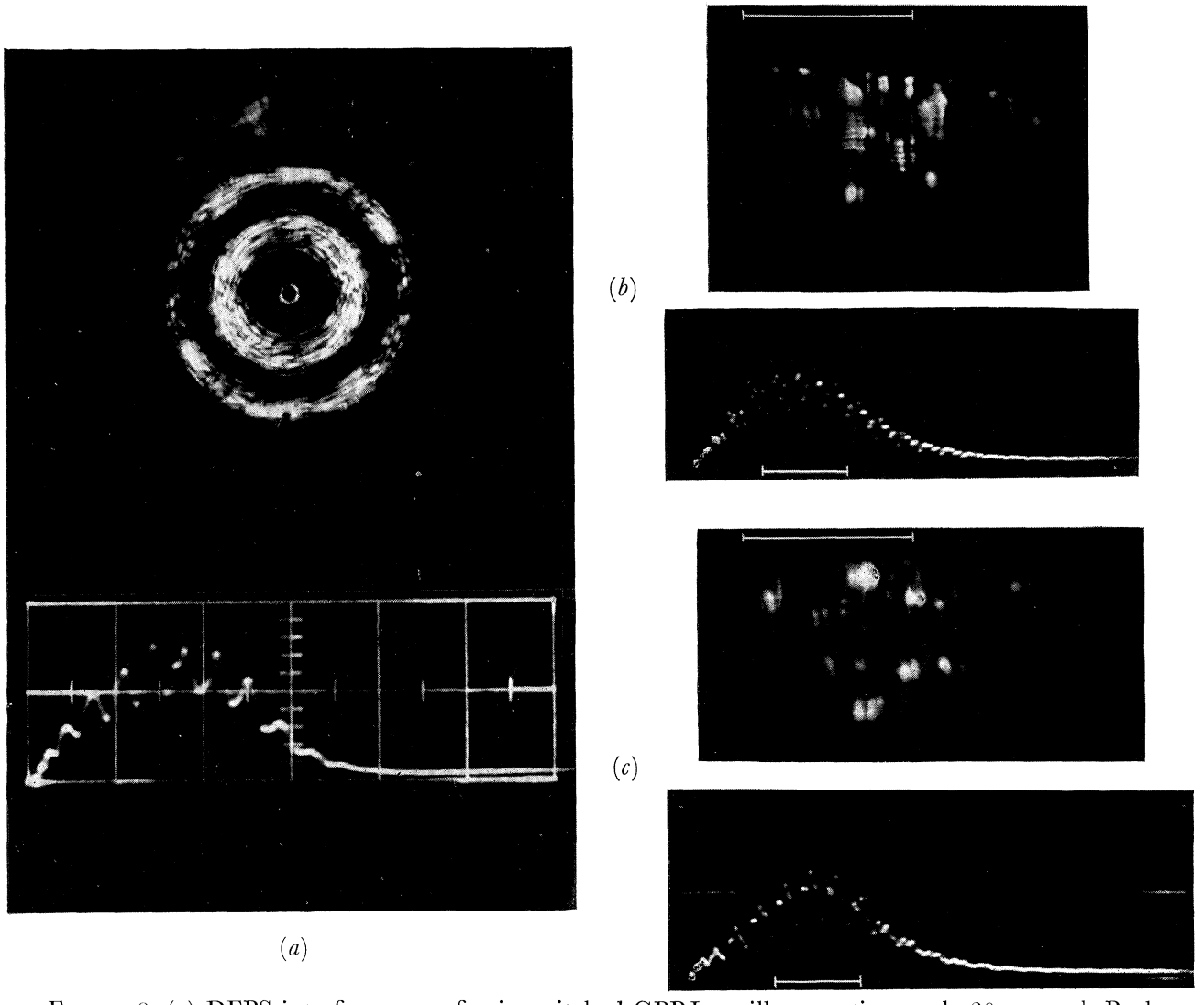

FIGURE 8. (*a*) DFPS interferogram of gain-switched GPRL oscillogram time scale 20 ns cm^{-1}. Peak power 5 MW. (*b*), (*c*). Image tube streak camera photographs of gain-switched GPRL beam cross-section. Streaking rate 1 ns mm^{-1}. Oscillograms time scale 20 ns cm^{-1}. Peak laser powers $\sim$ 4 MW. The scales represent 20 ns.

PHILOSOPHICAL TRANSACTIONS OF THE ROYAL SOCIETY A MATHEMATICAL, PHYSICAL & ENGINEERING SCIENCES

system (i). The system normally had two output reflectors of *ca.* 50 % reflectivity. Peak output power was in the form of two 50 MW beams for a total input of *ca.* 2000 J. Effective cavity length was 100 cm.

(iii) *Pockels-cell Q-switching plus saturable dye cell*

An antireflexion coated *Q*-switching (*ca.* 20 ns) Pockel cell, backed up by an isolator cell containing a weak solution of cryptocyanine in methanol, *Q*-switched a 4 in. $\times \frac{9}{16}$ in. fine ground ruby. Both plane parallel rod ends were anti-reflexion coated. The close coupled helical flash tube was cooled with circulating water. One end of the resonator cavity (effective length 100 cm) was formed by a roof-top prism and the output mirror had *ca.* 40 % reflectivity. Normal peak power was *ca.* 50 MW for input energies of 4000 to 4500 J.

All rubies used in the three systems were Linde superior internal quality (SIQ) of 0·05 % Cr^{3+} concentration.

Mode selection

The simplest means of mode selection were employed. The most effective, and common to all the systems under discussion, was found to be the resonant reflector first proposed by Kleinman & Kisliuk (1962). Two and three plate (optically contacted or mounted in Fabry–Pérot etalon type holders) resonators were used, of fused quartz or high refractive index glass, so as to produce the particular reflectivities required for the various laser systems. The effectiveness of a carefully designed resonant reflector in cleaning up a laser spectrum was demonstrated by the suppression of the above mentioned satellite lines generated in nitrobenzene Kerr-cell switches and amplified in the ruby active medium.

Additional mode selection could be achieved with cryptocyanine and other bleachable dyes, by inserting apertures, or by working close to threshold.

Results

Time integrated spectroscopy

With dielectric mirror output reflectors the spectral widths of all the systems tested were of the order 1 to 2 cm^{-1} for powers of 10 to 50 MW. With the appropriate resonant reflector this spectral width was in general reduced by more than an order of magnitude, for the same output power. This is because the number of modes which find a low loss, high reflectivity path, is sharply reduced. This is illustrated in figure 5*a*, *b*, plate 3, which show DFPS interferograms of the rotating prism system (i) employing (*a*) a dielectric mirror and (*b*) the equivalent resonant reflector. In the first case the number of spectral components is so large, and they are so closely spaced, that a diffuse uniform continuum is produced. For this system (i) (3 in. ruby) typical output power with a resonant reflector was *ca.* 5 MW in 0·12 cm^{-1} width with a beam divergence of *ca.* 2 mrad. For the gain switched system (ii) (11 in. of ruby) a total power of 20 MW in a spectral width of 0·012 cm^{-1} (360 MHz) was consistently obtained with specially designed resonant reflectors (Magyar 1967). Occasionally up to 40 MW of the same spectral purity were obtained (figure 5*c*).

PHILOSOPHICAL TRANSACTIONS OF THE ROYAL SOCIETY A MATHEMATICAL, PHYSICAL & ENGINEERING SCIENCES

Some typical DFPS interferograms of the three systems studied, with the respective pulse envelope oscilloscope traces, are shown in figures 5 and 6, plates 3 and 4. In all cases resonant reflectors were employed. Figure 5*d*, a typical output spectrum (photographed on Kodak IF film IR 135) of the rotating prism system (i), reveals complicated structure in the two main components which are themselves separated by five longitudinal mode spacings. At lower resolving power, particularly if Polaroid film was employed, these bands could appear as two separate longitudinal modes, each 200 to 250 MHz wide, i.e. much broader than the 10 MHz expected from the pulse duration transform. This spectral width is the same as that measured by McClung & Weiner and the DFPS interferogram confirms their hypothesis that the spectral broadening of apparently single longitudinal modes, is due to the presence of transverse components. With increasing pumping energy the time integrated spectrum tends to fill in until it appears as one broad band of fine structure.

Figure 8*a*, plate 6, is a typical spectrum of the gain switched system (ii). The longitudinal mode separation of 150 MHz is one-fifth of the 750 MHz free spectral range of the DFPS and the spectrum consists of many equal intensity components spread over *ca.* 250 MHz. These components, unlike the spectra of figure 6*a*, *b*, *c*, plate 4, do not form complete ring fringes. This indicates a complicated near field pattern, due to transverse mode structure or filamentary action of the laser rod, confirmed by time resolved photographs. (See below. Unlike the FPP, the DFPS is not translationally invariant in the laser beam and so any spatial structure is superposed on the ring pattern.) The pulse-envelope oscillogram is about 30 % modulated at a frequency corresponding to beating between two neighbouring longitudinal modes.

The advantages of uniform pumping, combined with a weak dye solution isolator, for obtaining very pure, low power, spectra is shown in figure 6*a*, *b*, *c*. The pockel cell switched system (iii) could be operated more easily at low power levels and generally gave a 'cleaner' spectrum. Near threshold output was spectrally very pure indeed and permitted the first direct spectroscopic detection of modes of single longitudinal, single transverse order in giant pulse lasers (Bradley *et al.* 1966*a*). Thus figure 6*a* shows three longitudinal modes, two of them neighbours. Figure 6*b*, two very narrow components separated by 40 MHz, compared with the longitudinal mode separation of 150 MHz, demonstrates the direct spectroscopic detection of pure transverse mode structure. Figure 6*c* shows a single mode with a measured line width of 10 MHz. The recorded spectral width is thus limited by the DFPS instrumental width of *ca.* 10 MHz, and the true line width must be very close to the pulse transform width of *ca.* 2·5 MHz. From the frequency difference between transverse modes given by interferograms such as figure 6*b*, the focal length of the thick lens, produced by the approximately spherical optical distortion due to nonuniform absorption of pump light by the plane parallel ruby rod (Townsend, Stickley & Maio 1965; Welling & Bickart 1966), can be easily calculated from the formulae of Stickley (1966) and Kogelnik (1965).

Despite the presence of the three longitudinal modes clearly recorded in the interferogram, the corresponding oscillogram gives no indication of beats at the expected frequencies, all of which fall within the 1 GHz detection bandwidth. Generally we have observed that there is little correlation between beat patterns and the corresponding

interferograms; the latter usually contain more modes than would be expected from the pulse envelope pattern. Single longitudinal mode operation cannot therefore be safely implied from the absence of beats alone. This is in agreement with the calculations of Statz & Tang (1965) who showed how the relative phases of longitudinal modes, and hence the degree of modulation of the pulse envelope, depend upon the location of the ruby within the cavity. Beats between two modes of different transverse order should not be observed when the full patterns of the modes fall on a photodiode of uniform cathode sensitivity. This is because the transverse mode functions form a complete orthogonal set (Kogelnik 1966). However, the presence of the above refractive index variations in the laser material would tend to remove the orthogonality (Stickley 1964).

Conversely, interferograms of well modulated pulse envelopes did not show clearly defined spectral components. Thus, while the oscillogram of figure 6*d* is nearly 100% modulated at 150 MHz, corresponding to the beat frequency of two neighbouring longitudinal modes, the interferogram consists of a broad fringe *ca.* 200 MHz wide. (The ring pattern is modulated by two-beam straight fringes (Bradley & Mitchell 1968) because the ruby was not lasing exactly collinearly with the He—Ne gas laser axis used for alining the DFPS. These fringes can be clearly seen in the centre of the interferogram.)

Because of these apparently anomalous results, time resolved spectroscopy with a fast image tube streaking camera was carried out.

Time resolved spectroscopy

Time resolution was achieved by streaking the etalon interferogram fringes with an STL image tube camera. Although the image tube had a S11 photocathode of low efficiency at the ruby laser wavelength (6943 Å), because of the intense illumination of the DFPS it was possible to record the streaked fringes at a writing speed of 2 ns/mm on 10 000 ASA Polaroid film employing a 1 mm streaking slit. Figure 7*a*, plate 5, a streaked spectrum of the gain switched GPRL, with the simultaneously recorded pulse envelope oscillogram, clearly shows a time and intensity dependent shift (Bradley *et al.* 1966*b*).

As expected from elementary considerations (Bradley *et al.* 1964), the interference fringes appear some 20 ns after the beginning of the light pulse. The intense broad 'fringe' near the centre of the pattern arises from a secondary focus of the exit, plano-concave, mirror substrate. Light of all frequencies from the whole aperture is focused here and it is interesting to note that the time modulation of this portion of the streaked photograph corresponds to that of the oscillogram. Thus time-resolved spectra and beats are simultaneously obtained, together with information on the spatial properties of the laser wavefront, from streaked DFPS interferograms. Figure 2 shows the expected time development of reflecting finesse N_R and peak fringe intensity of multiple-beam fringes, computed for a 40 cm optical path difference and mirrors of reflectivity 0·98, assuming a Gaussian input pulse of 35 ns halfwidth, representing a stationary range of frequencies.

N_R asymptotically approaches a value of 60, and the maximum fringe intensity is only 20% of the steady-state value. Since the relative intensities of the range of mode frequencies were changing within the duration of the giant pulse, the recorded finesses was much less (approximately 15 to 20). However, as can be seen from figure 7*a* the recorded fringes

do appear just before the peak of the laser giant pulse, in very good agreement with the computed prediction of figure 2.

Many streaked interferograms were recorded for a range of laser output powers. The most conspicuous feature of the fringes was a shift towards increasing diameter and thus decreasing frequency. For peak cavity powers of 5 to 10 MW the average shift was about 200 MHz and the apparent average lifetime of such a shifted fringe was about 20 ns. Usually a second fringe appears about 10 ns later, of the same initial diameter as that of the original fringe (figure 7*b*). At higher output powers several such cycles of fringes appear. Figure 3, a plot of the observed rate of frequency shift (fringe slope) as a function

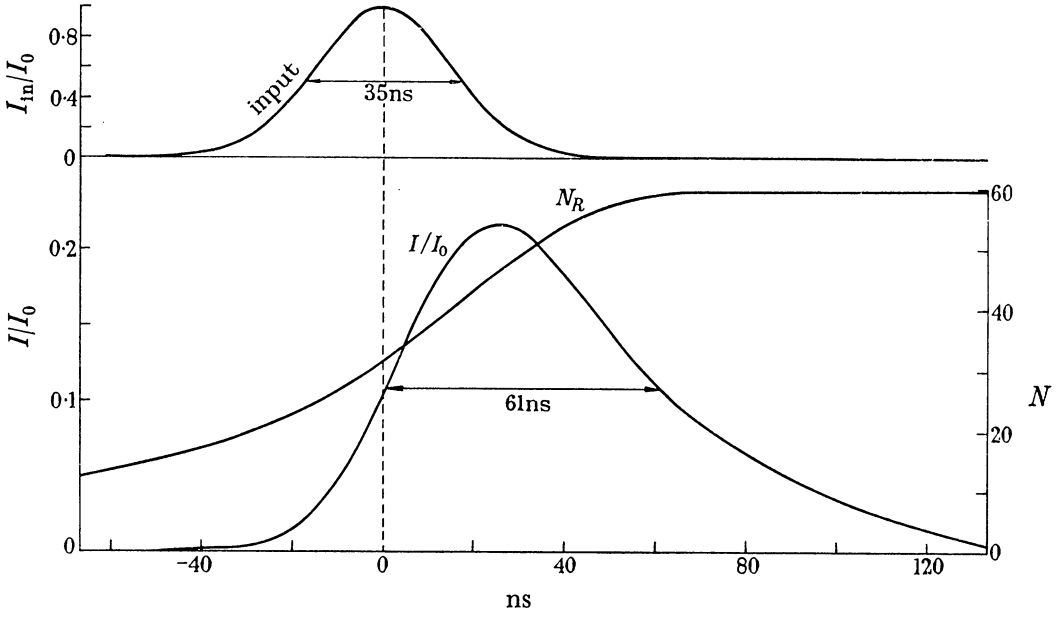

FIGURE 2. Time development of multiple-beam reflecting finesse, N_R, and peak fringe intensity for 40 cm optical path difference interferometer. Mirror reflectivity 0·98. Input pulse half-width 35 ns.

of peak cavity power, indicates an initial approximate linear relation, power dependent with a slope of 1·4 MHz ns^{-1} MW^{-1}. All the laser pulses had durations of 35 to 40 ns at the half-power level. Greater than average shifts usually occurred with more strongly temporally modulated giant pulses and vice versa. Taking into account the effect of this modulation on peak power leads to considerable reduction in the spread of the experimental points.

Figure 6*d* is now explicable since two longitudinal modes varying together in transverse mode order, could produce a well modulated pulse envelope while the time integrated DFPS interferogram would reveal only one broad spectral component. In general, for all laser systems studied, the more intense portions of the time integrated interferogram rings are broader, to be expected with an intensity dependent frequency shift. Since this shift limits the integrated spectral brightness obtainable from giant pulse ruby lasers, further experiments were carried out.

Frequency shifts in giant pulse ruby lasers

To further investigate laser time behaviour, streak photographs were taken of the laser beam cross-section as it appears in the plane of the DFPS interferometer. A 20 mm × 1 mm slit selected a suitable portion of the beam, which was then streaked at 1 ns/mm (1 ns time resolution). Two typical streak photographs are shown in figure 8*b*, plate 6. There is a definite transverse development of the active region, with time, and it is some 10 ns before lasing occurs along all of the slit length. The overall streak pattern is longitudinally modulated with the same periodicity as the oscillogram beats and transverse mode patterns are clearly discernible in the later stages of each *ca.* 10 ns cycle. To catch the beginning of the pulse an optical delay line of 28 m was needed and the streak photograph corresponds to only a small region of the laser beam cross-section, the centre of which may not coincide exactly with the mid-point of the slit.

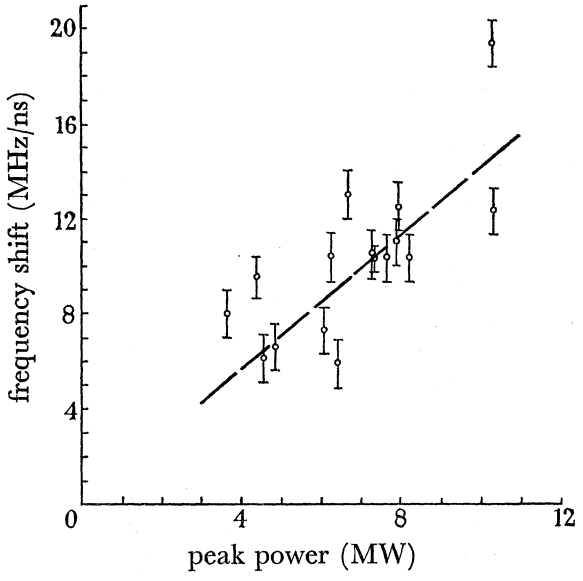

FIGURE 3. Plot of rate of frequency shift against laser power.

After this stage of the work was completed a blue shift (*ca.* 400 MHz), combined with a similar transverse development of the active region of a passive *Q*-switched ruby laser was reported (Korobkin, Leontovich, Popova & Shchelev 1966). Power dependence of the shift was not considered and the suggestion that laser heating could account for a decrease in the refractive index of the cryptocyanine, and thus in the optical length of the cavity, did not apply to our rotating prism giant pulse laser. A red shift of *ca.* 600 MHz from a vanadium phtalocyanine switched ruby laser, later reported (Orszag & Saron 1967), was explained by the combined effects of the intensity dependent anomalous dispersion of the phtalocyanine dye and the nonlinear susceptibility of the α-chloronaphthalene solvent, leading to an increase in refractive index of the required amount.

Intensity dependent blue shifts of *ca.* 400 MHz have also been recorded by us in the output of a Pockel's cell *Q*-switched *GPRL.* (3 in. × $\frac{3}{8}$ in. plane parallel ruby). Thus figure 7 (*c*), plate 5, shows a shift of 420 MHz in a 6 MW, peak cavity power, 80 ns pulse. Apart from the sign of the frequency change the time behaviour of the fringe pattern is very similar to that of figure 7 (*b*).

The approximate linear power relation suggested that these frequency shifts arise from a nonlinear optical electrical field effect in the ruby itself, producing directly refractive index changes with consequent changes in frequency, for constant mode order. The magnitude of the required change in refractive index can be easily obtained from the equation

$$2(nl_r+l_0) = m\lambda \tag{1}$$

for the wavelength λ corresponding to a longitudinal mode of order m of a plane parallel resonator, consisting of a ruby rod of length l_r and refractive index n, and an air path of length l_0.

Differentiation and rearrangement gives the relation

$$\delta n = -\frac{nl_r+l_0}{l_r}\frac{\delta\nu}{\nu}+\frac{\delta m}{2l_r}\frac{c}{\nu}. \tag{2}$$

Substituting our data ($l_r = 25$ cm, $l_0 = 56$ cm and $\nu = 4{\cdot}3\times10^{14}$ Hz) gives $\delta n = -1{\cdot}9\times10^{-6}$ for $\delta\nu = +200$ MHz for a 5 MW output pulse ($\delta n = 0$ for constant mode number).

Two possible nonlinear effects in ruby which could result in a rapid enough change in refractive index, of either sign, at the lasing frequency, are nonlinear anomalous dispersion (Javan & Kelley 1966), and the Bloch–Siegert, or optical frequency Stark effect (Davis 1963). Nonlinear anomalous dispersion could produce a maximum reduction in refractive index of 3×10^{-6} for a mode operating at the high frequency half-width point of the fluorescence line in an initially fully inverted ruby. For the operating conditions of our lasers, just above threshold, with an operating frequency near the fluorescence line centre, the effect is more than an order of magnitude too small (Berkeley & Wolga 1967). The Bloch–Siegert effect shift of the fluorescence line peak frequency ν_m leads to a positive frequency change given by

$$\Delta\nu_m = \mu^2E^2/4\nu_m h^2, \tag{3}$$

where μ is the electric dipole matrix element and E is the optical frequency electric field strength. Substituting the values $\mu = 1{\cdot}5\times10^{-20}$ (Nelson & Sturge 1965) and $E^2 \simeq 10^6$ e.s.u (assuming a 5 MW cavity power and a 1 mm active region) gives $\Delta\nu_m \simeq 10$ KHz. The subsequent change in refractive index at the lasing frequency, always negative unlike the direct anomalous dispersion effect, is again orders of magnitude too small, assuming a maximum total change of $0{\cdot}1$ cm^{-1} in gain during the giant pulse. Lattice strain in the ruby associated with population inversion has been postulated by Berkeley and Wolga to explain the increase with time, of the output frequency from a single spike of a ruby relaxation oscillator laser. A linear relationship is assumed between change in population inversion and change in optical length. Even if this is accepted extrapolating their results and calculations to our giant pulse laser gives an optical length change of one-tenth the correct magnitude.

Any change in the transverse mode order would also lead to a frequency shift. For a plane parallel cavity the resonant frequencies are given by (Kogelnik 1966)

$$\nu/\nu_0 = q+1+(1/\pi)\,(p+l+1)\,\cos^{-1}\sqrt{(G_1G_2)} \tag{4}$$

where q is the longitudinal mode order, ν_0 is the frequency spacing between two neighbouring longitudinal modes of the same transverse mode numbers p and l, and G_1 and G_2 are dimensionless parameters describing the optical design of the resonanator. Warter &

Martinelli (1966) have calculated that under transient conditions, nonlinear anomalous dispersion when combined with transverse variations of pumping, leads to distortion of low-order transverse modes of a laser cavity. The nett effect is to increase the gain of transverse modes on the high-frequency side of the fluorescence line centre relative to modes lying on or below the line centre. Physically the mode distortions are due to refraction of the laser field into regions where the refractive index is greatest. For mode frequencies above the line centre these are also the regions of greatest gain. These higher frequencies should then develop preferentially along the axis of a ruby rod where the population inversion is a maximum.

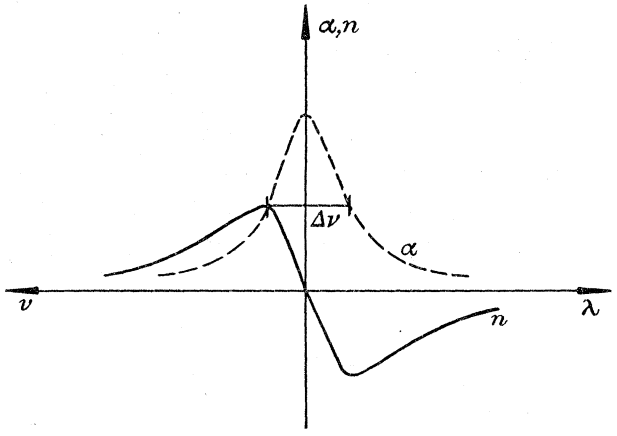

FIGURE 4. Frequency variation of gain α--- and refractive index n —— of an inverted ruby rod. Half-width of gain curve $\Delta\nu = 11\ \mathrm{cm}^{-1} = 3{\cdot}3 \times 10^{11}$ Hz.

Our time and intensity dependent frequency shifts and transverse development results can be explained by rapid bleaching of these initially active regions reversing the original transverse inversion gradients. For modes on the high frequency side of the line centre this leads to the generation of higher order transverse modes by beam spreading. Similarly beam narrowing would result in a red shift of modes on the low frequency side of the fluoresence line. Since the change in fractional inversion and peak power both increase with increasing initial inversion of the active region, and the duration of the 'local' giant pulse decreases (Wagner & Lengyel 1963) an intensity dependent rate of frequency shift is to be expected.

Comparison of figure 7*b*, plate 5 (2 MW pulse) with figure 7*a* (4 MW) clearly shows this intensity effect. For the first 8 ns of the low power pulse there is practically no frequency shift at all and lasing is confined to the central region of the fringe pattern as expected. (Because of the spatial resolution properties of the DFPS this is equivalent to examining the spectrum of a small region isolated by an aperture.) The 4 MW pulse lases along the whole slit length and the rate of frequency change is almost twice as great. The generation of a second longitudinal mode (figure 7*b*) after 12 ns is understandable in terms of spatial hole burning in the central region by the first mode (Tang, Statz & de Mars 1963). Calculation of the rate of frequency change would require a knowledge of the initial transverse inhomogeneities of inversion. In addition thermal inhomogeneities of the refractive index, due to heating of the ruby during pumping, would generally affect the values of the resonator parameters G_1 and G_2 of (4)

and thus the rate of frequency change. (The experimental determination of these variables is now being carried out for an exceptionally high optical quality ruby rod, symmetrically pumped by a helical flash tube.) An approximate formulae $\Delta\nu = c\theta^2/2\lambda$, relating the frequency change $\Delta\nu$ to the beam spread angle θ of a plane parallel Fabry–Pérot resonator, can be derived from geometrical optics. The maximum beam angle accepted by our spherical interferometer was 7×10^{-4} rad and substituting this gives $\Delta\nu$ of the order of 100 MHz, in good agreement with our experimental results.

Letokhov & Suchkov (1966) and Roess (1967) have considered theoretically the influence of an inhomogeneous distribution of inversion density on giant pulse evolution. While their calculated results are in qualitative agreement with the above simple physical model and with the results of our experiments, the effect of the inhomogeneous index of refraction was not included nor can a quantitative estimate of the rate of frequency change be obtained from their results. Ambartsumyan *et al.* (1967) have employed apertures and coaxial photocells to study the time development of the active region of a Kerr cell Q-switched ruby laser, obtaining results in good agreement with our streaked beam cross-section photographs. Frequency shifts were not measured by these authors.

Discussion

Time resolved interferograms and beam cross-section photographs have revealed a time dependence of both the output frequencies and the location of the active lasing regions of giant pulse ruby lasers. These results can be qualitatively explained by the combined effects of inhomogeneous distribution of inversion and nonlinear anomalous dispersion in the ruby. Time integrated interferograms can now be more easily interpreted and it is interesting to note that the mode lifetimes of between 2 and 8 ns predicted from the first interferograms of giant pulse ruby lasers (Bradley *et al.* 1963) are in excellent agreement with our present results. The discrepancies in the longitudinal mode separations then reported can now be understood in terms of differing transverse mode orders. Apparent discrepancies between spectra and beat patterns are also now removed and the danger of relying on beat patterns alone to obtain mode information has been demonstrated. It is clear that the spectral brightness of giant pulse lasers is limited by this inhomogeneous distribution of inversion and, as demonstrated, very pure spectral output can generally only be obtained at low output powers.

Experiments now under way (Bradley & McCullough, to be published) show that aperture mode selection when combined with compensation of the thermal distortion of the ruby rod, improves spectral purity. Again best results are obtained with uniform pumping (helical flash tube). Precise alinement, and adjustment of the ruby and aperture relative positions, is necessary.

The authors wish to thank Professor S. Tolansky, F.R.S., for his keen interest and support during the course of this research. We are glad to take this opportunity to express our gratitude to the Director, Dr R. S. Pease, and the Head of the Spectroscopy Division, Dr R. Wilson, of U.K.A.E.A. Culham Laboratory, for making available the laboratory facilities which made the extension of this work possible. Useful discussions with Dr D. E.

PHILOSOPHICAL TRANSACTIONS OF THE ROYAL SOCIETY A MATHEMATICAL, PHYSICAL & ENGINEERING SCIENCES

Evans, Mr M. J. Forrest, Dr J. Katzenstein and Dr M. Key are gratefully acknowledged. Thanks are also due to Mr R. Morrison who constructed the spherical mirror interferometer, and to Mr C. J. Mitchell for computing figure 2.

One of us (G. M.) was supported by a U.K.A.E.A. extra-mural research fellowship and two of us (M.S.E. and M.C.R.) were supported by S.R.C. studentships. Substantial assistance was received from the Science Research Council for the purchase of equipment and the provision of technical support.

References

Ambartsumyan, R. V., Basov, N. G., Zuev, V. S., Kryukov, P. G., Letokhov, V. S. & Shatberashvili, O. B. 1967 *Soviet Physics J.E.T.P.* **24**, 272.

Berkley, D. A. & Wolga, G. J. 1967 *J. Appl. Phys.* **38**, 3231.

Bradley, D. J., DeSilva, A. W., Evans, D. E. & Forrest, M. J. 1963 *Nature, Lond.* **199**, 1281.

Bradley, D. J., Bates, B., Juulman, C. O. L. & Majumdar, S. 1964 *Appl. Opt.* **3**, 1461.

Bradley, D. J., Engwell, M. S., McCullough, A. W., Magyar, G. & Richardson, M. C. 1966*a* *Appl. Phys. Lett.* **9**, 150.

Bradley, D. J., Magyar, G. & Richardson, M. C. 1966*b* *Nature, Lond.* **212**, 63.

Bradley, D. J., Magyar, G. & Richardson, M. C. 1966*c* *Proc. V Int. Conf. Phenomena in Ionised Gases*, **3**, 199. Belgrade: Gradevinska Knjiga Publishing House.

Bradley, D. J. 1967 *Nature, Lond.* **215**, 499.

Bradley, D. J. & Mitchell, C. 1968 *Phil. Trans.* A **263**, 209.

Connes, P. 1958 *J. Phys. Radium* **19**, 262.

Davis, L. W. 1963 *Proc. I.E.E.E.* **51**, 76.

Daneu, V., Sacchi, C. A. & Svelto, O. 1966 *I.E.E.E. J. Quant. Electr.* **QE-2**, 290.

Evans, D. E., Forrest, M. J. & Katzenstein, J. 1967 *Nature, Lond.* **212**, 21 (see other references listed by these authors).

Fritzler, D. & Marom, E. 1967 *Appl. Phys. Lett.* **11**, 16 (see other references listed by these authors).

Hellwarth, R. W. 1966 *Lasers* **1**, 283. London: Edward Arnold Ltd.

Javan, A. & Kelley, P. L. 1966 *I.E.E.E. J. Quant. Electr.* **QE-2**, 470.

Kleinmann, D. A. & Kislink, P. D. 1962 *Bell System Tech. J.* **41**, 453.

Kogelnik, H. 1965 *Bell System Tech. J.* **44**, 455.

Kogelnik, H. 1966 *Lasers* **1**, 320. London: Edward Arnold.

Korobkin, V. V., Leontovich, A. M., Popova, M. N. & Shchelev, M. Ya. 1966 *Soviet Physics J.E.T.P. Letters* **3**, 1944.

Letokhov, V. S. & Suchkov, A. F. 1966 *Soviet Physics J.E.T.P.* **23**, 763.

McClung, F. J. & Weiner, D. 1965 *I.E.E.E. J. Quant. Electr.* **QE-1**, 94.

Magyar, G. 1967 *Rev. Sci. Instr.* **38**, 517.

Nelson, D. F. & Sturge, M. D. 1965 *Phys. Rev.* **137** A, 1117.

Orszag, A. & Saron, R. 1967 *C.R. Acad. Sci., Paris* **264**, 1580.

Roess, D. 1967 *J. Appl. Phys.* **38**, 1705.

Statz, H. & Tang, C. L. 1965 *J. Appl. Phys.* **36**, 3923.

Stickley, C. M. 1964 *Appl. Opt.* **3**, 967.

Stickley, C. M. 1966 *I.E.E.E. J. Quant. Electr.* **QE-2**, 511.

Tang, C. L., Statz, H. & de Mars, G. A. 1963 *J. Appl. Phys.* **34**, 2289.

Townsend, R. L., Stickley, C. M. & Maio, A. D. 1965 *Appl. Phys. Lett.* **7**, 94.

Wagner, W. G. & Lengyel, J. 1963 *J. Appl. Phys.* **34**, 2040.

Warter, P. J. & Martinelli, R. U. 1966 *J. Appl. Phys.* **37**, 2103.

Welling, H. & Bickart, C. J. 1966 *J. Opt. Soc. Am.* **56**, 611.

PHILOSOPHICAL TRANSACTIONS OF THE ROYAL SOCIETY A MATHEMATICAL, PHYSICAL & ENGINEERING SCIENCES

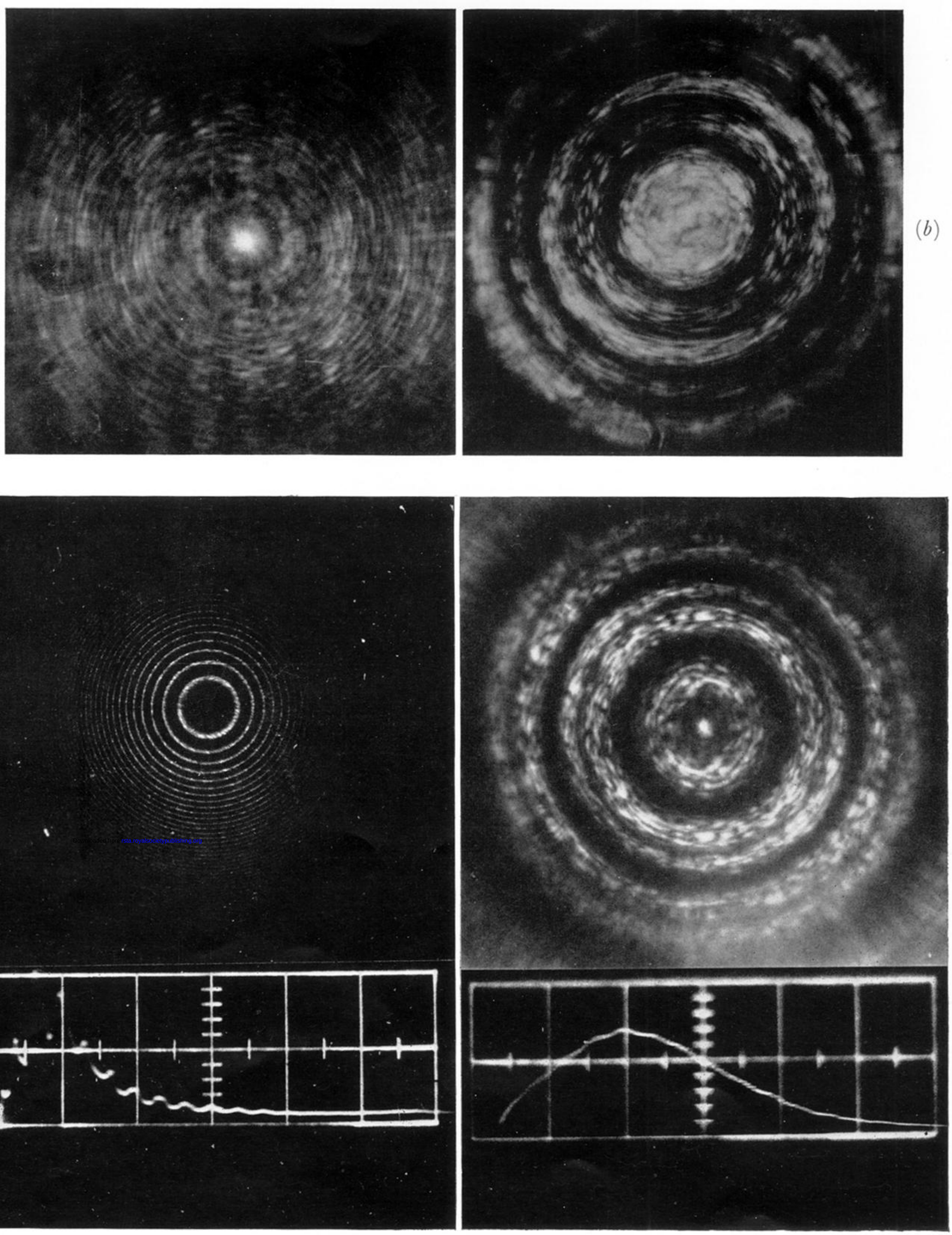

(a) (b) (c) (d)

FIGURE 5. (*a*, *b*). Comparison of the spectra of a rotating prism *Q*-switched GPRL taken with a spherical Fabry–Pérot interferometer for (*a*) 68 % reflectivity dielectric mirror (*b*) resonant reflector of same reflectivity. (*c*) Output spectrum of gain-switched rotating prism GPRL. Plane Fabry–Pérot interferogram. Free spectral range 1500 MHz. Oscillogram time scale 20 ns cm^{-1}. Peak power 40 MW. (*d*) Output spectrum of rotating prism system (i) FPS Interferogram. (Free spectral range 750 MHz.) Oscillogram time scale 20 ns cm^{-1}. Peak power 3 MW.

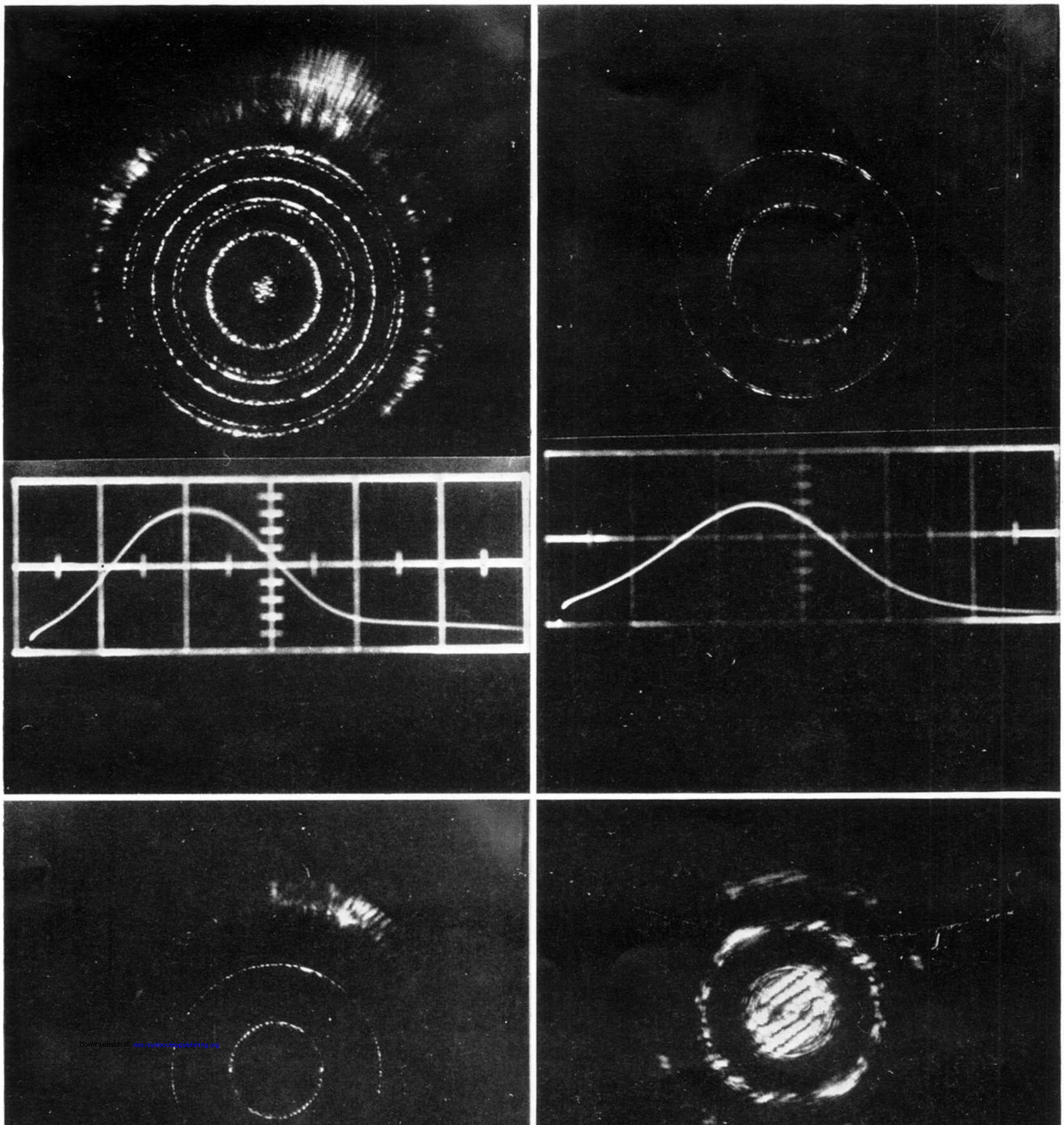

(a) (b) (c) (d)

FIGURE 6. (*a*) to (*c*). Output spectra of Pockel's cell *Q*-switched GPRL. DFPS interferograms. Oscillograms time scale 100 ns cm^{-1}. Peak powers ~ 100 kW. (*d*) DFPS interferogram of gain-switched rotating prism GPRL. Oscillogram time scale 20 ns cm^{-1}. Peak power 11 MW.

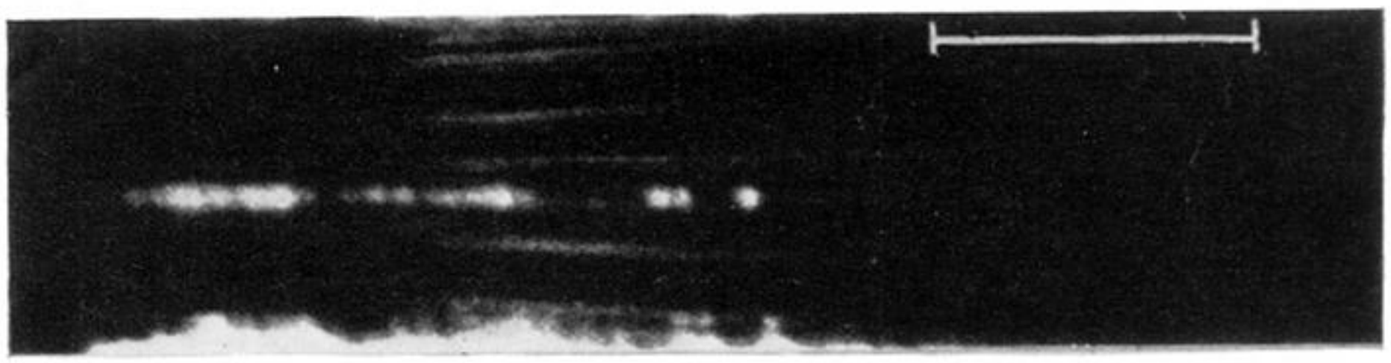

(*a*)

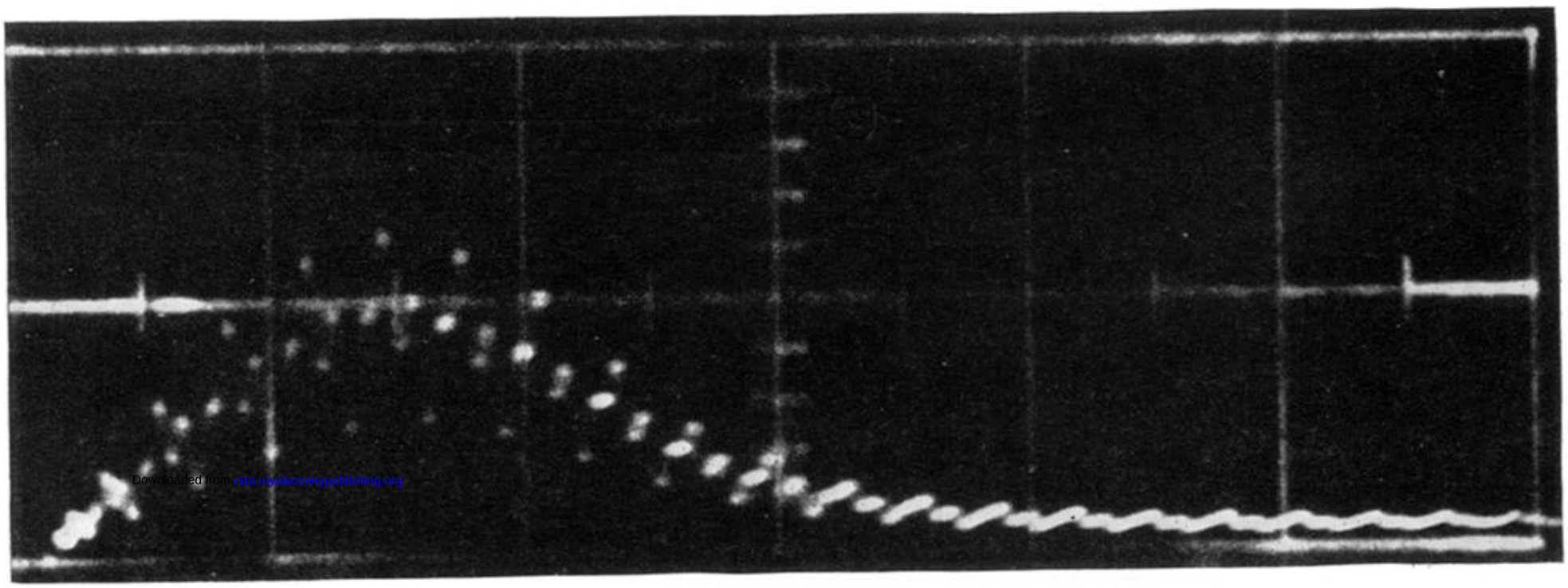

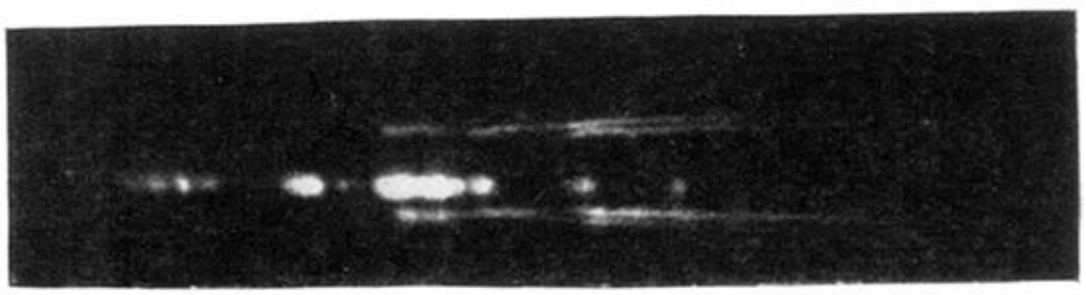

(*c*)

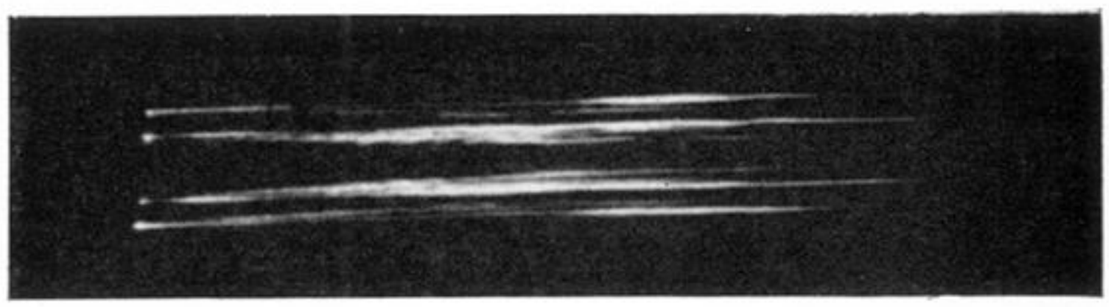

(*b*)

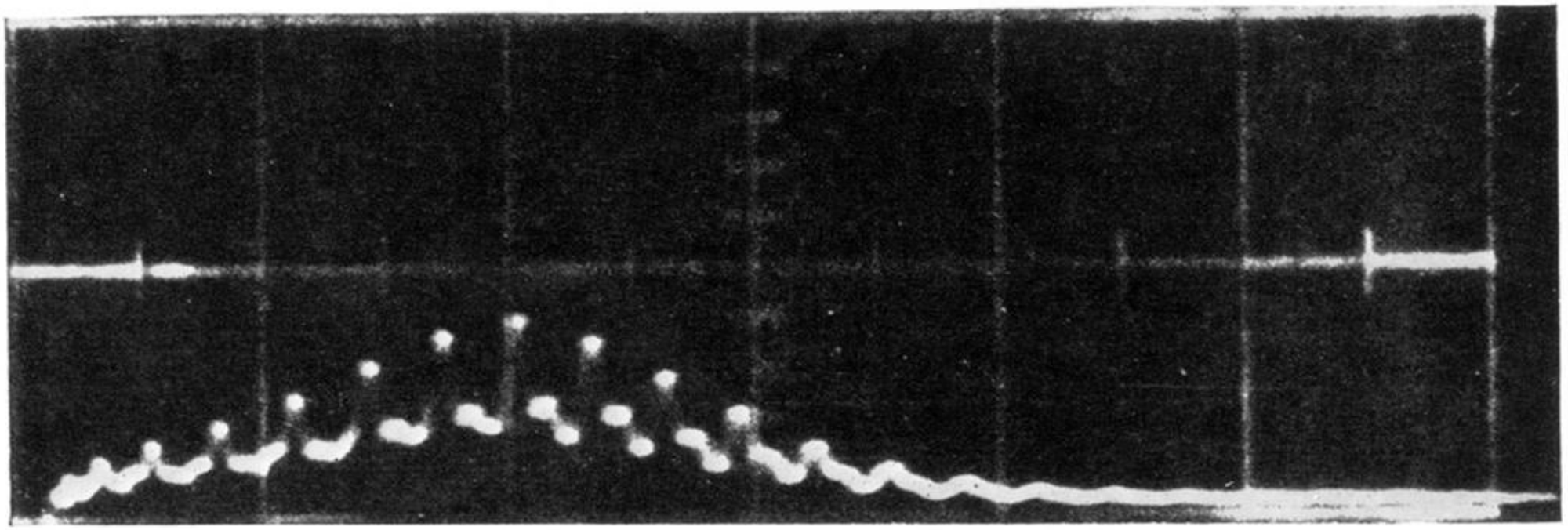

FIGURE 7. Streaked DFPS interferograms of (*a*, *b*) gain switched GPRL. Streak writing rate 2 ns mm^{-1}. Peak output powers (*a*) 4 MW, (*b*) 2 MW. Oscillogram time scale 20 ns cm^{-1}. (*c*) Pockel's cell GPRL. Peak output power 2 MW. Total streak time 200 ns.

PHILOSOPHICAL TRANSACTIONS OF THE ROYAL SOCIETY A MATHEMATICAL, PHYSICAL & ENGINEERING SCIENCES

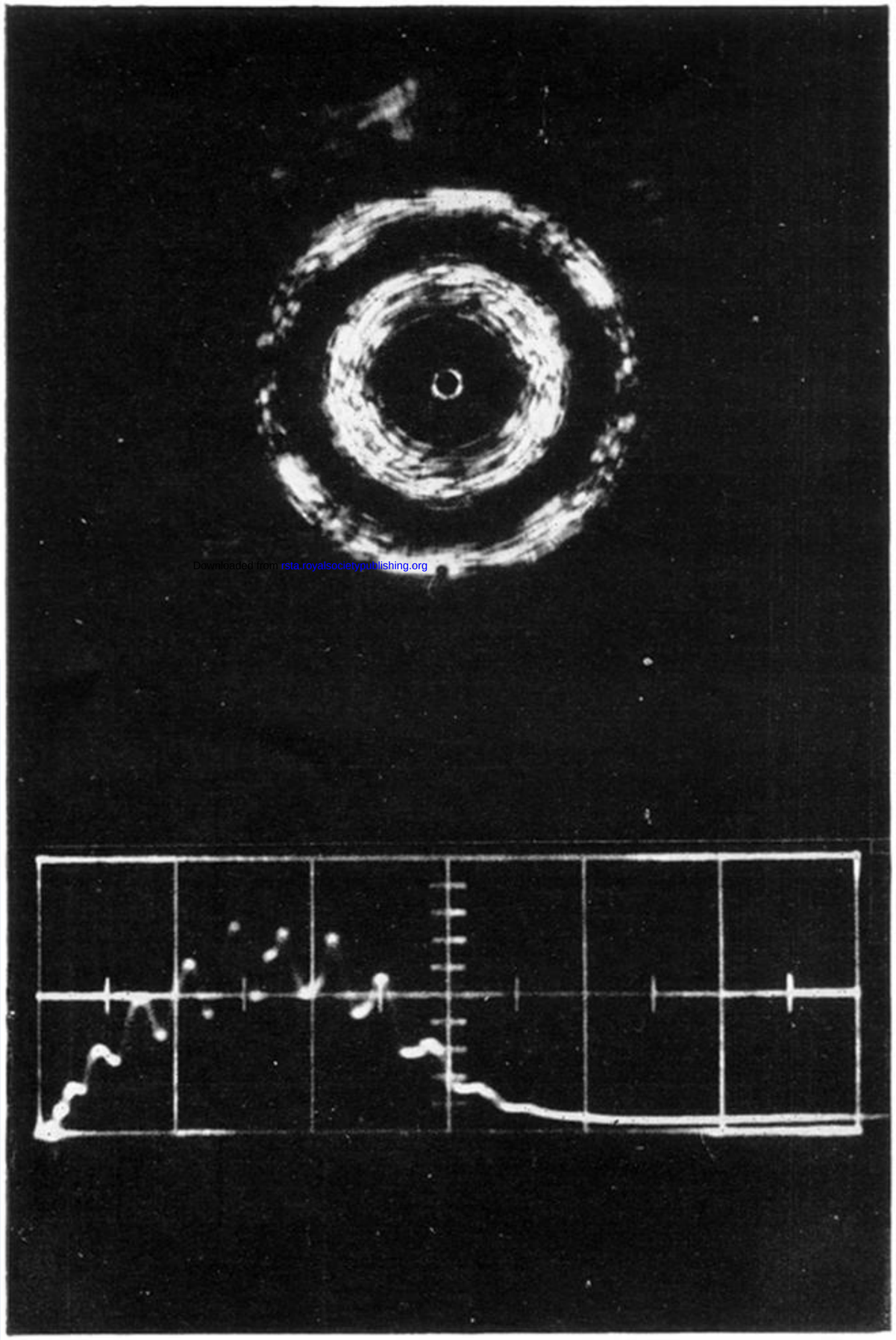

(a)

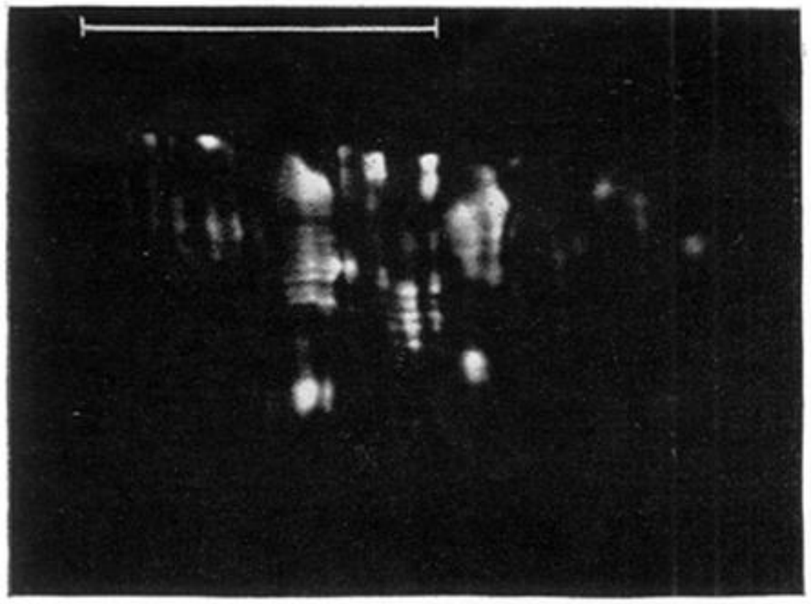

(b)

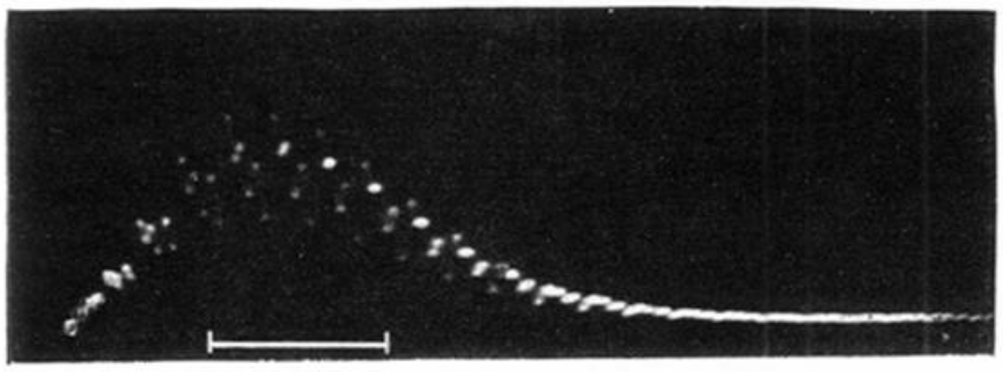

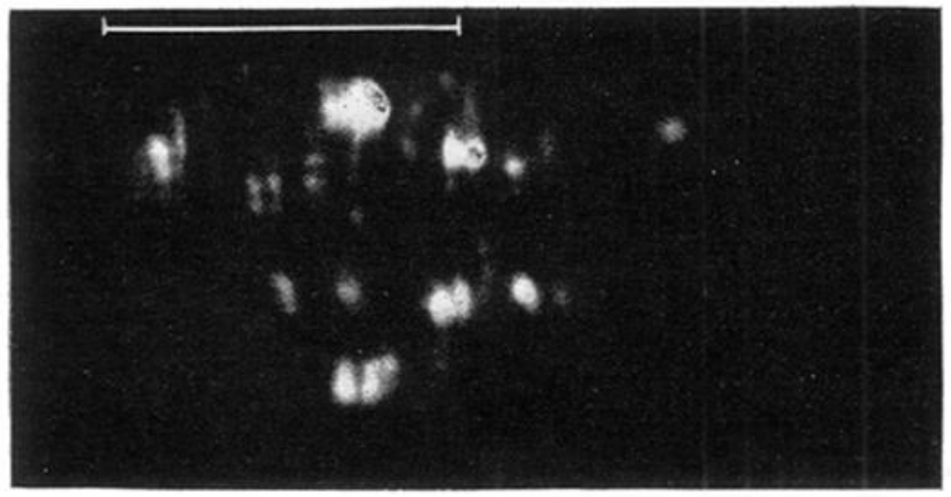

(c)

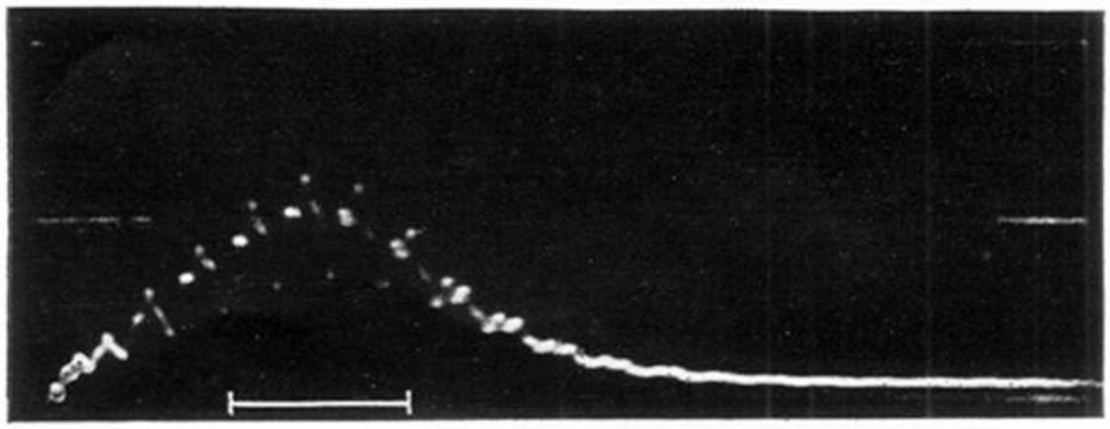

FIGURE 8. (*a*) DFPS interferogram of gain-switched GPRL oscillogram time scale 20 ns cm^{-1}. Peak power 5 MW. (*b*), (*c*). Image tube streak camera photographs of gain-switched GPRL beam cross-section. Streaking rate 1 ns mm^{-1}. Oscillograms time scale 20 ns cm^{-1}. Peak laser powers ~ 4 MW. The scales represent 20 ns.